# Vesicular Monoamine Transporter Substrate/Inhibitor Activity of MPTP/MPP$^+$ Derivatives: A Structure–Activity Study

D. Shyamali Wimalasena,[†] Rohan P. Perera,[†] Bruce J. Heyen,[‡] Inoka S. Balasooriya,[†] and Kandatege Wimalasena*,[†]

*Department of Chemistry, Wichita State University, Wichita, Kansas 67260-0051, and Department of Chemistry, Tabor College, Hillsboro, Kansas 67063*

*Received July 19, 2007*

The active metabolite of 1-methyl-4-phenyl-1,2,3,6-tetrahydropyridine (MPTP), *N*-methyl-4-phenylpyridinium (MPP$^+$), selectively destroys the dopaminergic neurons and induces the symptoms of Parkinson's disease. Inhibition of mitochondrial complex I and/or the perturbation of dopamine metabolism through cellular and granular accumulation have been proposed as some of the major causes of neurotoxicity. In the present study we have synthesized and characterized a number of MPTP and MPP$^+$ derivatives that are suitable for the comparative neurotoxicity and complex I inhibition versus dopamine metabolism perturbation studies. Structure−activity studies with bovine chromaffin granule ghosts show that 3′-hydroxy-MPP$^+$ is one of the best known substrates for the vesicular monoamine transporter (VMAT). A series of compounds that combine the structural features of MPP$^+$ and a previously characterized VMAT inhibitor, 3-amino-2-phenyl-propene, have been identified as the most effective VMAT inhibitors. These derivatives have been used to define the structural requirements of the VMAT substrate and inhibitor activities.

## Introduction

The neurotoxin, *N*-methyl-4-phenyl-tetrahydropyridinium (MPTP[a]), selectively destroys the dopaminergic neurons of the subatantia nigra and induces the symptoms of Parkinson's disease.[1–4] Numerous studies have shown that MPTP accumulates in the brain by crossing the blood brain barrier, and it is readily converted to the fully aromatized product, the *N*-methyl-4-phenylpyridinium salt (MPP$^+$), by monoamine oxidase. It has also been well accepted that the MPTP neurotoxicity is solely due to the metabolite MPP$^+$. In agreement with this proposal, direct administration of MPP$^+$ to the rat brain has been shown to specifically destroy the dopaminergic neurons. In addition, MPP$^+$ is shown to be taken up into dopaminergic neurons through the plasma membrane dopamine transporter (DAT) as well as into catecholamine storage vesicles through the granule vesicular monoamine transporter (VMAT).[1–4] Furthermore, MPP$^+$ inhibits oxidative phosphorylation by inhibiting complex I of the electron transport chain.[3] Although the exact mechanism of the specific toxicity of MPP$^+$ to dopaminergic neurons has not been fully understood, accumulating evidence suggests that at least two important characteristics of MPP$^+$ could be responsible for its toxic effects. While some studies suggest that the inhibition of complex I is the main cause, other studies appear to indicate that the perturbation of dopamine (DA) metabolism through cellular and granular accumulation may also play a role in the specific dopaminergic neurotoxicity of MPP$^+$.[4]

Although comparative structure–activity studies with respect to complex I inhibition versus DA metabolism perturbation by MPP$^+$ could provide valuable information to distinguish between the above two mechanisms, such detailed studies have not been carried out to our knowledge. In addition, accumulating experimental evidence indicates that the neurotoxicity of a large number of illicit drugs as well as other physicopharmacologically active agents may be due to the perturbation of catecholamine metabolism in the central nervous system (CNS).[5,6] Thus, the specific uptake of MPP$^+$ through DAT and its granular accumulation through VMAT also make it a convenient probe to study the in vivo effects of the perturbation of catecholamine metabolism. Similarly, properly designed MPP$^+$ derivatives could also be useful probes for the structure–activity studies of DAT and VMAT in vitro, since MPP$^+$ is a good substrate for the catecholamine uptake systems in plasma membrane and storage vesicles.[7,8] The structural rigidity of these derivatives in comparison to that of the regular phenylethylamine type substrates makes them ideal candidates for such studies. Based on these rationales, we have synthesized and characterized a number of MPTP and MPP$^+$ derivatives that are suitable for the structure–activity studies of DAT and VMAT as well as the comparative neurotoxicity and complex I inhibition versus DA metabolism perturbation studies. In the present paper we describe the synthesis and characterization of these derivatives and their use to define the structural requirements of the VMAT substrate and inhibitor activities using resealed chromaffin granule ghosts as a model.

## Results and Discussion

**Chemistry.** MPP$^+$ (**1**), MPTP (**15**), 2′-Me and 2′-NH$_2$ MPTP derivatives (**16–17**), and MPDP$^+$ClO$_4^-$ (**22**) were obtained from Sigma Aldrich. The 4′- and 3′-halo- (**7–9**), 4′-methyl- (**12**), 4′-methoxy- (**5**), and 4′- and 3′-trifluoromethyl- (**10−11**) MPP$^+$ derivatives were synthesized by the copper catalyzed coupling reaction between the appropriate ArMgBr derivative and an N-protected pyridine derivative followed by rearomatization of the pyridine ring by KMnO$_4$ and methylation of the pyridine nitrogen using methyl iodide (Scheme 1).[9,10] The hydroxy MPP$^+$

* To whom correspondence should be addressed. Phone: (316)-978-7386. Fax: (316)-978-3431. E-mail: kandatege.wimalasena@wichita.edu.

† Wichita State University.

‡ Tabor College.

[a] Abbreviations: APP, 3-amino-2-phenylpropene; ATP, adenosine triphosphate; CNS, central nervous system; DAT, plasma membrane dopamine transporter; DA, dopamine; HEPES, 4-(2-hydroxyethyl)-1-piperazine sulfonic acid; MPP$^+$, *N*-methyl-4-phenylpyridinium; MPTP, *N*-methyl-4-phenyl-1,2,5,6-tetrahydropyridine; MPDP, 1-methyl-4-phenyl-5,6-dihydropyridine; NE, norepinephrine; RES, reserpine; TBZ, tetrabenazine,VMAT, granule vesicular monoamine transporter(s); VMAT2, granule vesicular monoamine transporter-2.

10.1021/jm070875p CCC: $40.75 
Published on Web 01/26/2008

**Scheme 1.** Synthesis of 1-Methyl-4-phenylpyridinium Salts[a]

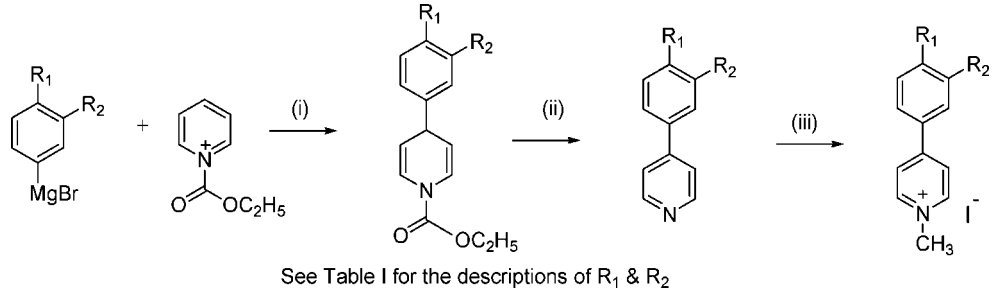


[a] (i) CuI/THF; (ii) $KMnO_4$/acetone, 0 °C, 15 min; (iii) $CH_3I$, THF, 0 °C.

**Scheme 2.** Synthesis of Hydroxy Derivatives of 1-Methyl-4-phenylpyridinium Salts[a]

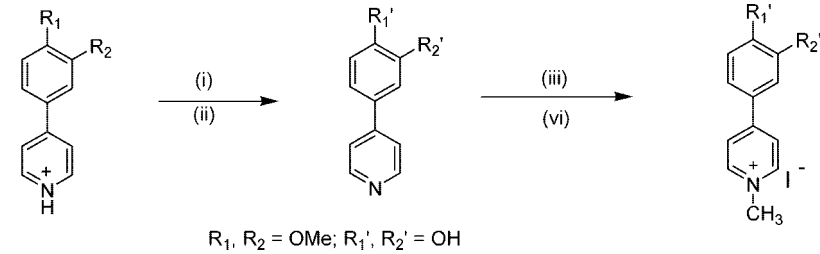


[a] (ii) Pyridine/HCl, 200 °C, 2−3 h; (ii) 1 M NaOH, 5 h; (iii) HCl, $NaHCO_3$; (iv) $CH_3I$, THF, 0 °C, 5 h.

**Scheme 3.** Synthesis of Hydroxy Derivatives of 1-Methyl-3-phenylpyridinium Salts (N3PP+)[a]

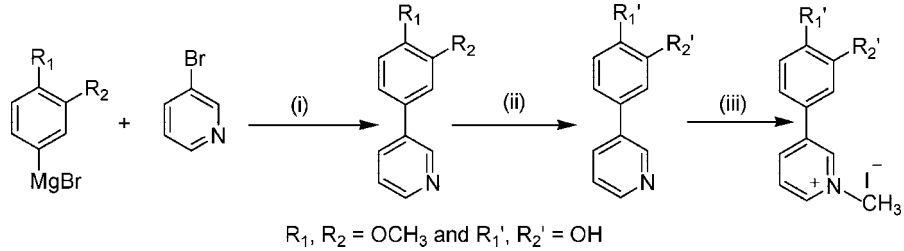


[a] (i) Dichlorobis(triphenyl-phosphine)nickel(II)/THF, 12 h; (ii) pyridine/HCl; (iii) $CH_3I$, THF, 0 °C, 5 h.

**Scheme 4.** Synthesis of 1-Methyl-4-phenyl-1,2,5,6 tetrahydropyridine (MPTP) Derivatives[a]

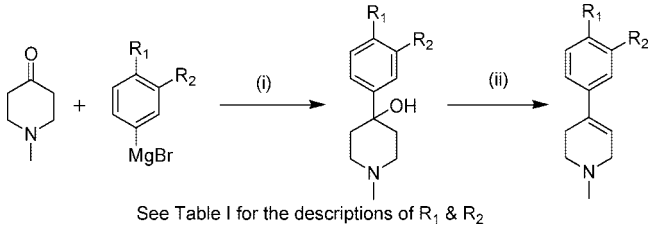


[a] (i) THF, room temperature, 12 h; (ii) 20% HAc in HBr, reflux 5 h.

**Scheme 5.** Synthesis of MPP+−APP Conjugates

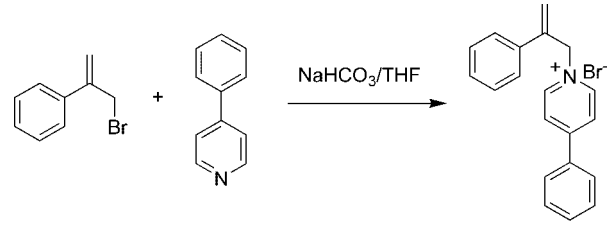


derivatives (**3**, **4**, and **6**) were prepared by the demethylation of the corresponding methoxy derivatives by using pyridine/HCl according to the procedure of Das et al.,[11] followed by methylation of the pyridine nitrogen by methyl iodide (Scheme 2). The 1-methyl-3-phenyl pyridinium salts (**13** and **14**) were synthesized from 3-bromo pyridine as shown in Scheme 3. The 1-methyl-4-phenyl-1,2,3,6-tetrahydropyridine (MPTP) derivatives (**18**–**21**) were synthesized by the Grignard reaction of 1-methyl-4-piperidone and the desired bromobenzene derivative, followed by a dehydration using 20% HAc in HBr under refluxing conditions (Scheme 4). The $MPP^+$-3-amino-2-phenylpropene conjugates (**23**–**31**) were prepared by nucleophilic displacement of $Br^-$ from the appropriate 3-bromo-2-phenylpropene derivative (Scheme 5).[12]

All new compounds were fully characterized and found to be highly stable in purified form. Under the biological assay (pH 7–7.5) or storage conditions, these compounds showed no tendency toward oxidation, polymerization, or hydrolytic cleavage of the N-substituents. Even under strong basic conditions (pH 12–14), compound **23** and its analogues showed no sign of hydrolysis of the pyridinium ring from the α-methyl styrene group. Compounds **23**–**28** were sparingly soluble in water and were freely soluble in polar organic solvents such as ethanol or DMSO. The concentrated stock solutions of those compounds were prepared in ethanol and used in all kinetic studies. However, the highest ethanol concentrations in the inhibition studies were kept to a minimum, usually less than 1%.

**Biological Studies.** Bovine adrenal chromaffin cells and their granules have been previously used in our laboratory to study DA uptake and conversion to norepinephrine (NE) and are proven to be effective models for the study of the granular

**Table 1.** Uptake and DA-Uptake Inhibition Kinetic Parameters of MPTP and $MPP^+$ Derivatives for Bovine Chromaffin Granule VMAT[a]

| inhibitor/substrate | $K_i$ ($\mu$M)[b] | $K_m$ ($\mu$M)[c] | $V_{max}$ (nmols/mg·min)[c] | $K_{m,DA}/K_{i,I}$[d] |
|---|---|---|---|---|
| **$MPP^+$ Derivatives** | | | | |
| $MPP^+I^-$ (**1**) | 92 ± 14 | 73 ± 11 | 1.4 ± 0.1 | 0.3 |
| 2′-$MeMPP^+I^-$ (**2**) | 95 ± 10 | | | 0.3 |
| 3′-$OHMPP^+I^-$ (**3**) | 2.4 ± 0.1 | 8.4 ± 2.1 | 1.9 ± 0.1 | 9.7 |
| 4′-$OHMPP^+I^-$ (**4**) | 82 ± 11 | 107 ± 16 | 1.6 ± 0.1 | 0.7 |
| 4′-$OMeMPP^+I^-$ (**5**) | 106 ± 14[e] | 135 ± 9 | 1.6 ± 0.1 | 0.2 |
| 3-Me-4′-$OHMPP^+I^-$ (**6**) | 65 ± 19[e] | | | 0.8 |
| 4′-$FMPP^+I^-$(**7**) | 51.3 ± 6.3[e] | | | 1.0 |
| 4′-$ClMPP^+I^-$ (**8**) | 7.6 ± 0.7 | | | 5.8 |
| 3′-$ClMPP^+I^-$ (**9**) | 46.3 ± 5.4[e] | | | 1.1 |
| 4′-$CF_3MPP^+I^-$ (**10**) | 33.8 ± 4.2[e] | | | 1.3 |
| 3′-$CF_3MPP^+I^-$ (**11**) | 24.6 ± 3.0[e] | | | 1.8 |
| 4′-$CH_3MPP^+I^-$ (**12**) | 51.8 ± 8.7 | 41.3 ± 6.6 | 0.9 ± 0.1 | 1.0 |
| 4′-$OHN_3PP^+I^-$ (**13**) | 338 ± 142 | | | 0.1 |
| 3′-$OHN_3PP^+I^-$ (**14**) | 36.6 ± 4.3[e] | | | 1.2 |
| **MPTP Derivatives** | | | | |
| MPTPHCl (**15**) | 52.5 ± 6.3 | 409 ± 88 | 1.7 ± 0.3 | 0.5 |
| 2′-MeMPTPHCl (**16**) | 38.4 ± 5.2 | | | 0.7 |
| 2′-$NH_2$MPTPHCl (**17**) | 193 ± 39[e] | | | 0.1 |
| 3′-OHMPTP HCl (**18**) | 25.8 ± 3.1[e] | | | 1.7 |
| 4′-OHMPTP HCl (**19**) | 134 ± 24[e] | | | 0.3 |
| 3′-ClMPTP HCl (**20**) | 27.7 ± 3.4 | | | 1.6 |
| 4′-F MPTP HCl (**21**) | 49.7 ± 6.3[e] | | | 0.9 |
| $MPDP^+ClO_4^-$ (**22**) | 53.0 ± 13.6[e] | | | 0.7 |

[a] Uptake and DA-uptake inhibition kinetics were determined using resealed chromaffin granule ghosts under standard uptake conditions as previously described.[12–14] Resealed granules ghosts were prepared from frozen membrane stores prior to the kinetic experiment and used immediately. The kinetic parameters were determined for each derivative using the same ghost preparation, but different preparations were used for different derivatives. [b] The $K_i$ values were obtained by fitting the experimental data (typically four to five different inhibitor and six different DA concentrations) to the Cleland's COMP program.[23] All inhibitions were competitive with respect to DA. The ± values were standard errors obtained from fitting routines. [c] The $K_m$ and $V_{max}$ values for various substrates were determined by fitting the initial uptake rates at 12 different concentrations of the substrate to the hyperbolic form of the Michaelis−Menten equation. [d] The $K_{m,DA}/K_{i,I}$ ratios were calculated from the respective $K_{i,I}$ and $K_{m,DA}$ parameters determined for each compound in order to normalize the variation of $K_m$ for DA for difference ghost preparations. [e] $K_i$ values were estimated by fitting the experimental data (obtained at 0 and 200 $\mu$M inhibitor and 6 different DA concentrations) to the standard competitive inhibition equation using Sigmaplot (Cambridge Software Corp.).

**Table 2.** Structures and VMAT Inhibition Kinetic Parameters of $MPP^+$−APP Conjugates

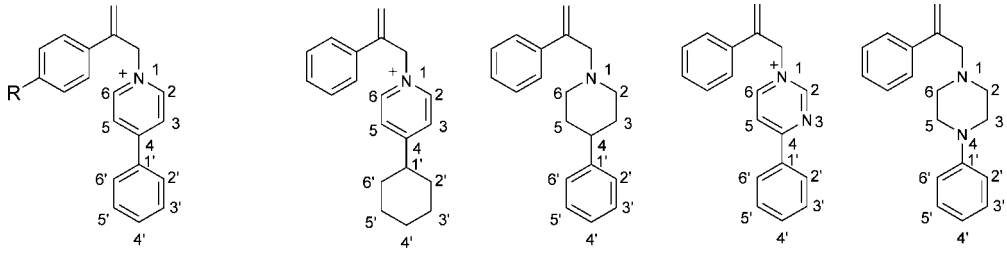


| inhibitor | $K_i$[a] ($\mu$M) | $K_{m,DA}/K_{i,I}$[b] | inhibitor | $K_i$[a] ($\mu$M) | $K_{m,DA}/K_{i,I}$[b] |
|---|---|---|---|---|---|
| **23** | 38.4 ± 4.2 | 0.9 | **28** | 2.8 ± 0.1 | 8.7 |
| **24** | 53.0 ± 13.6 | 0.7 | **29** | 0.4 ± 0.1 | 55 |
| **25** | 16.4 ± 2.7 | 1.8 | **30** | 0.5 ± 0.1 | 41.5 |
| **26** | 13.4 ± 1.7 | 2.7 | **31** | 4.5 ± 0.5 | 11.3 |
| **27** | 1.4 ± 0.2 | 24.1 | | | |

[a] $K_i$, inhibition kinetics was determined in resealed chromaffin granule ghosts under standard uptake conditions as detailed in Table 1. All inhibitions were competitive with respect to DA. The ± values were standard errors obtained from fitting routines. [b] The $K_{m,DA}/K_{i,I}$ ratios were calculated from the respective $K_{i,I}$ and $K_{m,DA}$ parameters determined for each compound in order to normalize the variation of $K_m$ for DA for difference ghost preparations as in Table 1.

metabolism of catecholamines.[12–14] The relevance of chromaffin granule model studies to the central nervous system catecholamine storage vesicles is substantiated by the finding that bovine adrenal chromaffin granules express the same brain specific VMAT2 as the major transmembrane monoamine transporter.[15] We have previously reported the experimental protocols to examine the kinetics of uptake and conversion of intragranular DA to NE by using resealed bovine chromaffin granule ghosts without using radiolabeled substrates, and we have also shown that the resealed chromaffin granules are a good model system to study the structure–activity of VMAT2.[12–14] As previously reported,[12] minor variations of uptake kinetics between day to day ghost preparations could be normalized using the kinetic parameters determined for the DA uptake with the same ghost preparations. Therefore, the $K_{m,DA}/K_{i,I}$ ratio is a more accurate parameter in estimating the relative inhibition potencies of VMAT inhibitors for more quantitative purposes. However, as evident from the data in Tables 1 and 2, these variations are relatively small, and the intrinsic $K_i$ parameters could still be used in qualitative analysis of the kinetic data. Thus, we have used bovine chromaffin granule ghosts as a model to characterize a number of novel MPTP and $MPP^+$ derivatives

with respect to their interactions with the VMAT to determine their suitability as DA perturbation probes.

Proper granular storage of catecholamines is highly critical for the functioning of the catecholaminergic nervous system. Perturbation of granular accumulation of catecholamines has been recognized as a major factor in the physicopharmacological and neurotoxic toxic effects of a large number of illicit drugs.[5,6] In spite of this convincing evidence, little attention has been paid to understand the molecular details of the accumulation and storage of catecholamines in storage vesicles through the VMAT. For example, in contrast to the earlier proposal that the unprotonated form of amines is the only form transported through the VMAT, the finding that the quaternary ammonium salt $MPP^+$ is also effectively transported under physiological conditions led to the proposal that protonated amine may be the substrate for the VMAT.[7,8] Apart from this information very little is known about the specificity, the molecular nature of the interaction of the substrates or inhibitors, or the mechanism of the amine transfer through the VMAT. Although highly potent well-known inhibitors such as reserpine, tetrabenazine, and ketanserin have been extensively used in biochemical and pharmacological studies of the VMAT,[16–18] their application in structure–activity studies has been limited due to the following: (a) nonspecific interaction with the membrane lipids altering the integrity of the membrane, (b) very tight binding to the transporters, (c) low solubility in the experimental medium, (d) structural complexity, and so forth. Therefore, development of specific inhibitors and/or alternate substrates that may be conveniently used in the structure–function and mechanistic studies of VMATs is a significant goal. We have previously characterized a series of 3-amino-2-phenyl-propene (APP) derivatives as novel and simple reversible inhibitors for the bovine chromaffin granule VMAT.[12] In the present study, we have taken advantage of the VMAT substrate and inhibitor activities of $MPP^+$ and 3-amino-2-phenyl-propene (APP) derivatives, respectively, to develop and characterize a series of probes, and we have used them to further define the structure–activity relationships of the substrates and inhibitors of the VMAT.

**Structure–Activity Studies.** Previous studies have suggested that 1-methyl-4-phenyl pyridinium (**1**, $MPP^+$) is a good substrate for resealed chromaffin granular ghost VMAT.[7,8] However, the data presented in Table 1 clearly show that it is a relatively weak substrate, in comparison to DA. Similarly, most $MPP^+$ derivatives tested were also weak substrates for the VMAT, except the 3′-OH derivative (**3**). While this derivative is an excellent substrate with a $K_m$ of 8.4 ± 2.1 μM and a $V_{max}$ of 1.9 ± 0.1 nmols/mg·min, the 4′-OH derivative (**4**) was a very weak substrate (Table 1), which is unexpected, since both 4′- and 3′-tyramines are almost equally good substrates for VMAT (D. S. Wimalasena and K. Wimalasena, unpublished observations). In contrast to $MPP^+$ derivatives, all of the MPTP derivatives tested were found to be very weak or not substrates for the VMAT.

The inhibition kinetics of substituted $MPP^+$ derivatives show that **3** very effectively competes with DA for uptake under the standard conditions ($K_i$ = 2.4 ± 0.1 μM). It interacts with the VMAT about 10 times better than DA and about 35 times better than the parent compound, $MPP^+$ (**1**, $K_i$ = 92 ± 14 μM), under similar experimental conditions. In addition, the $K_m$ determined for **3** under standard uptake conditions was about 4 times greater than the $K_i$ determined by DA competition experiments (Table 1), suggesting that it is a kinetically sticky substrate for the VMAT; that is, the rate constant for the dissociation of the transporter−**3** complex is significantly slower than that of the transport ($k_{-1} < k_2$). These findings suggest that the 3′-OH group of **3** may play a critical role in the interaction with the VMAT, which parallels the effect of 3′-OH substitution on 3-amino-2-phenyl-propene (APP) derivatives.[12] In contrast to the high inhibition potency of **3**, the 4′-OH derivative (**4**) does not compete effectively for VMAT and showed a weaker inhibition potency ($K_i$ = 82 ± 11 μM), which is consistent with its weak substrate activity. However, this behavior sharply contrasts the effects of the 4′-OH substitution in APP inhibitors.[12] Strikingly, 4′-Cl substitution (**8**) also increased the inhibition potency of the parent compound significantly. Although not experimentally verified, the efficient competition of this derivative (**8**) with DA for uptake suggests that it could probably be a good substrate for VMAT as well.

Among the MPTP derivatives tested, the 3′-OH derivative (**18**) appeared to be the best competitive inhibitor for VMAT with respect to DA uptake, which further confirmed the importance of the 3′-OH group in the inhibition as well as the VMAT substrate activities of both series of compounds. However, the inhibition potency of **18** is about 10 times weaker than that of the corresponding $MPP^+$ derivative (**3**). Interestingly, the inhibition potencies of MPTP as well as some of its derivatives (for example **16** and **20**) are higher than those of the corresponding $MPP^+$ derivatives, suggesting that they interact well with the transporter in spite of poor substrate activities. Thus, the transport through the VMAT appears to require more stringent molecular interactions than the inhibition. The above results also suggest that the 3′-OH groups of both $MPP^+$ and MPTP play an important role in the interaction with the VMAT. A similar trend is also apparent with the 3′-$CF_3$ in the $MPP^+$ series. Therefore, the 3′-substituents of these two classes of compounds may play a critical role in the interaction with the VMAT through H-bonding with an amino acid residue in the binding site. However, in contrast to the regular phenylethylamine VMAT substrates, the 4′-OH groups of $MPP^+$ or MPTP do not contribute significantly to the substrate activity or the inhibition potencies. On the other hand, bulky hydrophobic substituents at the 4′-position, specifically halogen, positively contribute to the binding, similar to the trend that was observed with previously characterized APP inhibitors.[12]

To further exploit the interaction of these derivatives with the VMAT, we have designed, synthesized, and characterized a series of probes that mimic the structural features of both APP (a previously characterized inhibitor[12]) and $MPP^+$ (substrate). The uptake studies with granule ghosts have shown that the prototypical parent derivative, the $MPP^+$−APP conjugate (**23**), was not detectably taken up even at the 200–500 μM concentrations, suggesting that the bulky substituent (2-phenylpropene) on nitrogen completely abolishes the VMAT substrate activity of $MPP^+$. However, **23** was found to be a reasonably good competitive inhibitor for the VMAT with a $K_i$ of 38 ± 4 μM (Table 2). Comparison of the inhibition potency of **23** with that of **1** indicates that the bulky hydrophobic substituent on the nitrogen significantly enhances the inhibition potency of $MPP^+$. Based on these findings, a number of structurally distinct APP−$MPP^+$ conjugates were synthesized and characterized, and their VMAT inhibition potencies were determined. These studies have revealed that the replacement of the 4-phenyl group of the parent compound (**23**) with a cyclohexyl group (**24**) decreases the inhibition potency ($K_i$ = 53.0 ± 13.6 μM), suggesting that the planar aromatic ring at the 4-position of the pyridine ring of these conjugates plays a favorable role in the interaction with the transporter. However, the replacement of

the pyridine ring with a piperidine or pyrimidine ring (**25**, **26**) increased the inhibition potency noticeably ($K_i$ = 16.5 ± 2.7 and 13.4 ± 1.7 $\mu$M, respectively). More importantly, the replacement of the pyridine ring with a piperazine ring (**27**) increased the inhibition potency even more significantly. Thus, piperazine derivative **27** is approximately 25-fold more potent than the parent compound **23** and about 10–11-fold more potent than the piperidine- or pyrimidine-based inhibitors **25** and **26**. These findings appear to indicate that the piperazine ring binds more favorably to the transporter than the planar pyridinium ring of conjugate inhibitors. We believe these interesting differences could be due to the relatively high flexibility of the piperazine ring in comparison to the pyrimidine ring of **26** [the presence of an additional nitrogen atom on the ring may also positively contribute to the inhibition potency of this derivative (see below)]. In addition, these findings appear to indicate that the permanently charged quaternary ammonium functionality of $MPP^+$ derivatives is not mandatory and/or optimal for the effective interaction with the transporter, which is consistent with our finding that MPTP is a better inhibitor than $MPP^+$ for VMAT (see below).

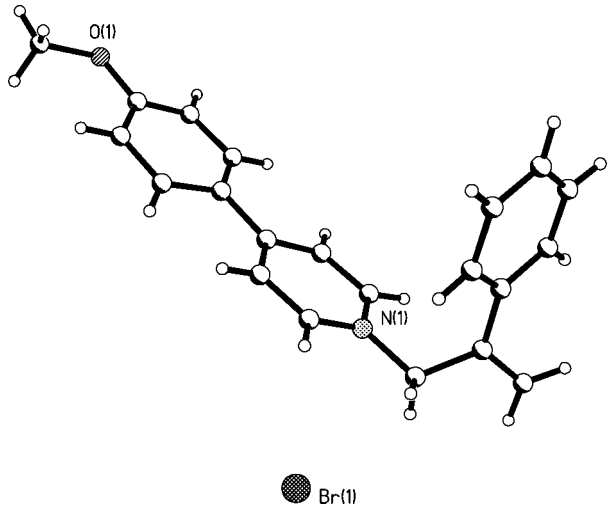


**Figure 1.** Crystal structure of **28**.

To determine the distinct roles of the $MPP^+$ and APP portions of the above conjugates in the interaction with the VMAT, a series of APP−$MPP^+$ conjugates with different substituents on the $MPP^+$ phenyl ring have been synthesized and examined. These studies revealed that substitution of a 4′-OMe on the phenyl ring of the conjugate (**28**) increases the inhibition potency by about 14-fold compared to the parent compound (**23**). This result is quite opposite of the effects observed in 4′-OMe substitution on the substrate/inhibitor activities of $MPP^+$ itself (Table 1). Introduction of a 3′-OH on the $MPP^+$ phenyl and a 4′-I on the 2-phenyl propene moieties of the parent conjugate (**29**) (previous studies have shown that bulky hydrophobic halogens on the 4′-position of APP derivatives significantly enhance their inhibition potencies[12]) increases the inhibition potency significantly, and this was the most potent conjugate inhibitor ($K_i$ = 0.44 ± 0.05 $\mu$M) discovered in the present study. However, again in contrast to the trend observed in substrate activities, 4′-OH substitution also increases the inhibition potency of the conjugates to a level very similar to that of the 3′-OH substitution (**30**). These drastic differences in substituent effects between the inhibition potencies of $MPP^+$ and the conjugates appear to suggest that the $MPP^+$ portion of the conjugate inhibitors may interact with the transporter in a slightly altered fashion in comparison to $MPP^+$ itself.

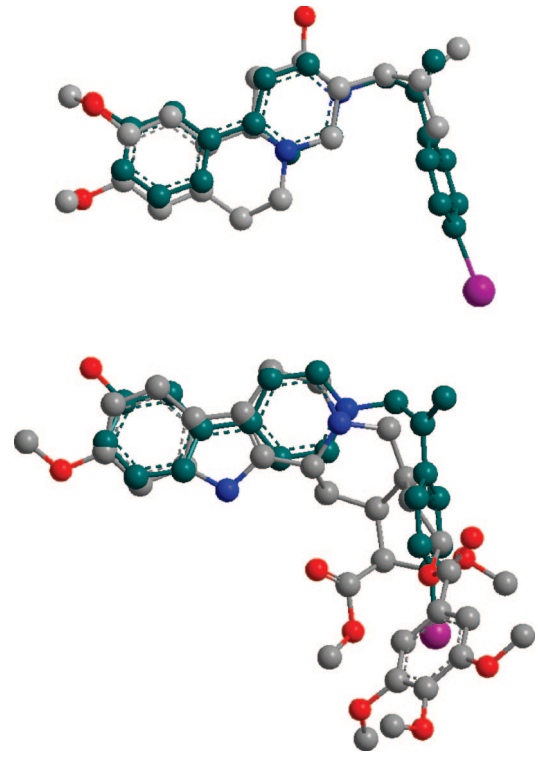

**Figure 2.** Overlay of energy minimized structures of tetrabenazine with **29** (top) and reserpine with **29** (bottom).

The above results suggest that the $MPP^+$ portion of the above conjugates may largely determine their inhibition properties and the APP portion could play an auxiliary role, presumably through nonspecific hydrophobic interactions. This proposal is supported by the finding that the addition of an extra phenyl group to the 2-phenyl propene moiety of the parent conjugate (**31**) significantly enhanced the VMAT inhibition potency ($K_i$ = 4.5 ± 0.5 $\mu$M). It is also consistent with our previous observation that the inhibition potency of the 4′-halogen substituted APP derivative increases with the increasing hydrophobicity of the halogen (I > Br > Cl > F).[12] Furthermore, the crystallographic analysis of the structures of these derivatives (the structure of **28** is shown in Figure 1; this derivative gave X-ray quality crystals readily, in comparison to the most potent inhibitor, **29**) shows that these molecules possess a well-defined "L" shape architecture, and both the APP and $MPP^+$ portions may interact with the VMAT as two separate entities, leading to higher inhibition potencies in comparison to those of either of the two derivatives.

Computer modeling studies show that the $MPP^+$−APP conjugates structurally resemble the known potent VMAT inhibitors reserpine (RES) and tetrabenazine (TBZ) (Figure 2). Overlay of the optimized structures of **29** and TBZ shows that the two molecules are structurally similar with respect to steric constraints and positioning of the 4′- and 3′-phenyl ring oxygen substituents. However, the ring nitrogens could not be fully overlaid keeping the above constraints intact, indicating that the nitrogens of the VMAT bound **29** and TBZ may not occupy the same positions of the active site. Similar modeling studies with RES show that the nonaromatic nitrogen of RES and the pyridine nitrogen of **29** superimpose well (Figure 2), suggesting that they could occupy similar positions in the binding site. These proposals are consistent with the finding that the replacement of the pyridine ring of the $MPP^+$ portion of **23**

with nonaromatic piperidine (**25**) or piperazine (**27**) increases the inhibition potency significantly. Thus, the high affinity of TBZ ($K_i \sim 4$ nM) in comparison the $MPP^+$−APP conjugates could be due to the optimal positioning of the nitrogen and the carbonyl oxygen (which is not present in $MPP^+$−APP conjugates or RES) in the binding site. We note however that the large trimethoxyphenyl tail of RES could not be mimicked by TBZ or any of the above $MPP^+$−APP conjugate inhibitors. Thus, since the carbonyl oxygen is not present and the nitrogens of RES may not contribute toward optimal binding, its extended hydrophobic tail must provide a significant contribution toward its high binding affinity, especially since the binding site of the transporter is shown to be highly hydrophobic. This proposal is further supported by the previous report that the trimethoxyphenyl acetate-cleaved RES derivative, reserpic acid, is at least a 2000-fold weaker inhibitor than RES (the $K_i$'s of RES and reserpic acid are 1–7 nM[19] and 10 $\mu$M,[20] respectively). Since the above conjugates may not have optimal positioning of the nitrogen and also may lack an extended hydrophobic tail, they are substantially weaker inhibitors for VMAT in comparison to TBZ and RES, but they are comparable to reserpic acid. The excellent substrate activity of 3′-OH $MPP^+$ (probably the best known substrate for the VMAT) in comparison to the 4′-OH $MPP^+$ and DA shows that the relative positioning of 3′-OH with respect to the pyridine nitrogen in $MPP^+$ derivatives is optimal for the VMAT substrate activity. Thus, the similar inhibition potencies observed for the $MPP^+$−APP conjugates with respect to 3′- and 4′-OH further indicate that the mode of interaction of these as well as RES and TBZ inhibitors with the transporter could be distinct from that of regular substrates.

Based on the above findings, a hypothetical working model is proposed for the interaction of substrates and inhibitors of the VMAT. The salient features of the model are as follows: (a) substrate transport through the VMAT requires much more stringent interactions than the inhibition, (b) the orientation of the 3′-OH with respect to the pyridine nitrogen of $MPP^+$ (**3**) is optimal for substrate activity in contrast to regular phenylethylamine substrates, (c) the interaction of $MPP^+$−APP conjugates as well as TBZ and RES may not precisely mimic the mode of substrate interaction, (d) the $MPP^+$−APP conjugates, TBZ, and RES may interact with the transporter in a similar mode, and (e) the nitrogen and carbonyl functionalities of TBZ and the trimethoxyphenyl hydrophobic tail of RES may contribute significantly to their high inhibition potencies.

As mentioned above, the conjugate inhibitors characterized in the present study are significantly weaker than the commonly employed classical inhibitors such as RES and TBZ. However, structural simplicity and well-defined structural rigidity together with the easy synthetic accessibility of these derivatives make them more appealing for systematic structure–activity studies. On the other hand, they share some common limitations that are associated with those classical inhibitors such as low solubility and nonspecific membrane interactions. Further structural refinements of these inhibitors for better inhibition potencies and increased solubilities are currently underway.

## Conclusions

A series of MPTP and $MPP^+$ derivatives have been designed, synthesized, and characterized as novel substrates/inhibitors for the VMAT. The 3′-OH derivative of $MPP^+$ has been identified as one of the best known substrates for the VMAT. Comparative structure–activity analysis of these inhibitors and substrates suggests that the VMAT substrate activity must satisfy much more stringent structural requirements than the inhibition. The wide variability of the VMAT substrate and/or the inhibitory activities of these simple derivatives make them highly desirable probes to examine the molecular mechanisms pertinent to the neurotoxicity of $MPP^+$. The most effective inhibitors identified in the present study were a series of compounds that integrate the structural features of $MPP^+$ and APP, a previously characterized VMAT inhibitor.[12] The overall structures of these $MPP^+$−APP conjugates were remarkably similar to the well-known classical VMAT inhibitors RES and TBZ. The structure–activity analysis of these three series of inhibitors supports a proposal that the high inhibition potency of TBZ could be due to the optimal placement of the ring nitrogen and carbonyl oxygen in the active site, and in the case of RES, nonoptimal nitrogen interactions and the lack of a corresponding carbonyl oxygen may be compensated by the contributions from the hydrophobic trimethoxyphenyl tail. We believe this information would enable the design and synthesis of potent and structurally simple inhibitors for monoamine transporter(s) for further structure–activity studies. In addition, the comparative toxicological studies of the $MPP^+$ derivatives and conjugates characterized in the present studies should also be useful in determining the underlying mechanisms responsible for the specific dopaminergic neurotoxicity of $MPP^+$. These studies are currently underway in our laboratory.

## Experimental Section

**A. Materials.** All reagents and solvents were obtained from various commercial sources with the highest purity available and used without further purification. Tetramethylsilane (for deuterated organic solvents) or 3-(trimethylsilyl)propionic acid sodium salt (for $D_2O$) was used as internal standard for $^1H$ NMR. Beef liver catalase (65 000 units/mg protein) was obtained from Boehringer−Mannheim. Protein assay reagents were obtained from Bio-Rad laboratories. The compounds $MPP^+I^-$ (**1**), MPTPHCl (**15**), 2′Me-MPTPHCl (**16**), 2′$NH_2$-MPTPHCl (**17**), and $MPDP^+ClO_4^-$ (**22**) were obtained from Sigma Aldrich.

**B. General Methods.** All $^1H$ and $^{13}C$ NMR spectra were recorded on a Varian Inova 400 or 300 MHz spectrometer, and mass spectra were obtained from a Finnigan LCQ-Deca ion trap mass spectrometer (Thermoquest Corporation, San Jose, CA). All melting points were uncorrected and determined using MEL-TEMP II (Laboratory Devices, USA). All of the elemental analyses were carried out by Desert Analytics (Tucson, AZ). Compounds **5** and **7** have been previously synthesized and characterized.[10] Compounds **2**, **8**−**12**, **18**−**20**, **25**−**27**, and **30** are structurally simple and related to the analytically fully characterized parent compounds. Therefore, their structural conformations and purities were assessed by "clean" $^1H$ and $^{13}C$ NMR spectra, mass spectrometry, and $C_{18}$-reversed phase HPLC.

**C. Computational Calculations.** Ab initio calculations were carried out using the *Gaussian 98-Revision A.9* suite[21] of programs. The overlay of minimized structures was carried out by using the built-in overlay function of Chem 3D Ultra (CambridgeSoft, Cambridge, MA).

**D. Chromaffin Granule Isolation.** Chromaffin granules were prepared as previously described with minor modifications.[12–14] Fresh bovine adrenal glands were dissected, and medullary tissue was collected in ice cold 0.3 M sucrose, 10 mM HEPES buffer, pH 7.0. The tissues were homogenized with a Biospec biohomogenizer, and the homogenate was centrifuged at 3600 rpm (1200*g*) for 10 min at 4 °C. The resulting supernatant was centrifuged at 18 000 rpm (27 000*g*) at 4 °C for 25 min; the supernatants were discarded. The pellets were washed carefully by swirling with ~1–2 mL of 0.3 M sucrose, 10 mM HEPES buffer, pH 7.0 to remove the white fluffy upper layer. The washed pellets were resuspended in the above buffer and homogenized using a Potter-Elvejhem homogenizer, and the above centrifugation and washing steps were repeated. The pellets were resuspended in 0.3 M sucrose, 10 mM

HEPES buffer, pH 7.0, and homogenized, and the homogenate was layered on 1.6 M sucrose, 10 mM HEPES buffer, pH 7.0, and then centrifuged at 27 500 rpm (58 700*g*) for 90 min at 4 °C. The pellets were washed and resuspended in lysing buffer containing 0.2 M tris phosphate buffer, 100 $\mu$g/mL catalase, pH 7.0, and glycerol (7:1 v/v) and homogenized. The lysed granules were stored at −70 °C.

**E. Biological Evaluation.** All kinetic experiments were carried out using properly characterized resealed bovine chromaffin granule ghosts as previously described.[12–14] Briefly, the washed granule membranes isolated from the above stores were resealed to contain 20 mM Tris phosphate, 100 mM KCl, 150 mM sucrose, 10 mM fumarate, and 100 $\mu$g/mL catalase (pH 7.0) and were purified by a discontinuous Ficoll/sucrose density gradient. The resealed granule ghosts were incubated in a medium (0.5 mL total volume) containing 0.3 M sucrose, 10 mM HEPES, 5 mM Mg−ATP, 5 mM $MgSO_4$, and 100 $\mu$g/mL catalase, (pH 7.0) at 30 °C for 10 min (uptake conditions). Then, the desired concentrations of the inhibitor were added to the mixture, which was incubated further for 2 min. Following the incubation period, the uptake reaction was initiated by the addition of the desired concentration of DA, and 400 $\mu$L aliquots of the incubate were withdrawn at 6 min time intervals and diluted into 5.0 mL of ice cold 0.4 M sucrose, 10 mM HEPES, pH 7.0. These samples were then centrifuged at 36 000*g* for 25 min at 4 °C, the supernatants removed, the pellets gently washed three times with 0.4 M sucrose, 10 mM HEPES, pH 7.0, and the tubes swabbed dry. Then, 500 $\mu$L of 0.1 M $HClO_4$ was added, the pellets were homogenized, and the extraction was allowed to proceed for 20 min at room temperature. After low speed centrifugation to remove coagulated protein, the catecholamines in the acidic extracts (intragranular catecholamines) were separated and quantified by reversed phase HPLC-EC. In uptake experiments, the same procedure was used, except that DA was excluded from the incubations and the intragranular levels of various substrates were quantified by HPLC-UV.

**F. Synthesis. 1. Technical Statement.** Due to potential health hazards of $MPP^+$ and MPTP and related derivatives, extreme caution should be taken in their synthesis and use. The guidelines for proper handling of MPTP derivatives have been reported.[22]

**2. Synthesis of 1-Methyl-4-phenyl Pyridinium Salts.** These compounds were synthesized according to the procedure described by Das et al. with minor modifications (Scheme 1).[9] To a suspension of anhydrous CuI (0.3 g, 1.5 mM) and dry pyridine (0.04 mol) in dry THF (100 mL) was added ethyl chloroformate (0.03 mol) under $N_2$, at −30 °C, and the reaction mixture was stirred for 30 min. Then, a solution of Grignard reagent (0.04 mol) prepared from the respective phenyl bromide and Mg turnings in THF (100 mL) was added dropwise over 15 min. The mixture was stirred for 15 min at −30 °C and then at room temperature until the solution became clear (in some cases the solution was refluxed for 10 h under $N_2$ to obtain a clear solution). Then, the reaction mixture was treated with saturated $NH_4Cl$ (50 mL), extracted with ether, dried with $Na_2SO_4$, and concentrated, and the resultant dihydropyridine intermediate was oxidized by dropwise addition of $KMnO_4$ in acetone at 0 °C (until the pink permanganate color persisted for several minutes). After evaporation of acetone, the brown solid was suspended in ether and filtered. The ether solution was washed several times with 5% $NaHCO_3$, dried over $Na_2SO_4$, and concentrated under vacuum. The free base was dissolved in anhydrous THF and treated with MeI at 0 °C to give the corresponding quaternary ammonium salt, which was crystallized using ethanol/ether.

**a. 1-Methyl-4-(2′-methylphenyl)pyridinium Iodide (2).** Yield 41%; mp 226–228 °C; $^1$H NMR ($D_2O$) $\delta$ 2.17 (s, 3H), 4.24 (s, 3H), 7.24–7.26 (m, 4H), 7.86 (d, 2H), 8.60 (d, 2H); $^{13}$C NMR ($D_2O$) $\delta$ 20.4, 48.5, 127.3, 130.3, 132.9, 1343.9, 135.9, 136.5, 147.2, 148.2, 158.9; MS (ESI) *m/z* 184.11 ($M^+$).

**b. 1-Methyl-4-(4′-methoxyphenyl)pyridinium Iodide (5).** Yield 42%; mp 226–228 °C; $^1$H NMR ($D_2O$) $\delta$ 2.42 (s, 3H), 4.32 (s, 3H), 7.38 (d, 2H), 7.70 (d, 2H), 8.09 (d, 2H), 8.61 (d, 2H); $^{13}$C NMR ($D_2O$) $\delta$ 41.3, 49.5, 126.3, 130.3, 132.9, 133.9, 146.2, 147.2, 157.9; MS (ESI) *m/z* 200.1 ($M^+$).

**c. 1-Methyl-4-(4′-fluorophenyl)pyridinium Iodide (7).** Yield 38%; mp 231–234 °C; $^1$H NMR ($D_2O$) $\delta$ 4.31 (s, 3H), 7.19 (d, 2H), 7.45 (t, 2H), 8.19 (q, 2H), 8.58 (d, 2H); $^{13}$C NMR ($D_2O$) $\delta$ 50.0, 119.2, 119.4, 127, 132.2, 132.9, 133, 144.4, 157.1, 166.2, 168.7; MS (ESI) *m/z* 188.09 ($M^+$).

**d. 1-Methyl-4-(4′-chlorophenyl)pyridinium Iodide (8).** Yield 32%; mp 225 °C; $^1$H NMR ($D_2O$) $\delta$ 4.32 (s, 3H), 7.38 (d, 2H), 7.30 (d, 2H), 8.09 (d, 2H), 8.61 (d, 2H); $^{13}$C NMR ($D_2O$) $\delta$ 50.1, 130.3, 132.9, 146.2, 147.2, 157.9; MS (ESI) *m/z* 207.12 ($M^+$).

**e. 1-Methyl-4-(3′-chlorophenyl)pyridinium Iodide (9).** Yield 34%; mp 226–228 °C; $^1$H NMR ($D_2O$) $\delta$ 4.34 (s, 3H), 7.54−7.64 (m, 4H), 8.19 (d, 2H), 8.63 (d, 2H); $^{13}$C NMR ($D_2O$) $\delta$ 50.0, 127.5, 128.9, 130.3, 133.6, 134.2, 137.5, 138.2, 147.6, 157.3; MS (ESI) *m/z* 207.12 ($M^+$).

**f. 1-Methyl-4-(4′-trifluorophenyl)pyridinium Iodide (10).** Yield 38%; mp 236–237 °C; $^1$H NMR ($D_2O$) $\delta$ 4.31 (s, 3H), 7.84 (d, 2H), 8.12 (d, 2H), 8.28 (d, 2H), 8.32 (d, 2H); $^{13}$C NMR ($D_2O$) $\delta$ 50.0, 126.53, 131.2, 133.9, 134.1, 148.1, 148.9, 157.4, 162.4; MS (ESI) *m/z* 238.09 ($M^+$).

**g. 1-Methyl-4-(3′-trifluorophenyl)pyridinium Iodide (11).** Yield 23%; mp 218–221 °C; $^1$H NMR ($D_2O$) $\delta$ 4.31 (s, 3H), 7.34−7.51 (m, 4H), 7.82 (d, 2H), 8.51 (d, 2H); $^{13}$C NMR ($D_2O$) $\delta$ 50.0, 119.1, 129.4, 126, 128.2, 131.3, 134.3, 143.4, 155.1, 159.2, 164.7; MS (ESI) *m/z* 238.09 ($M^+$).

**h. 1-Methyl-4-(4′-methylphenyl)pyridinium Iodide (12).** Yield 46%; mp 216–219 °C; $^1$H NMR ($D_2O$) $\delta$ 2.43 (s, 3H), 4.32 (s, 3H), 7.38 (d, 2H), 7.70 (d, 2H), 8.09 (d, 2H), 8.61 (d, 2H); $^{13}$C NMR ($D_2O$) $\delta$ 22.3, 49.8, 126.3, 130.9, 132.2, 132.8, 146.1, 147.2, 157.9; MS (ESI) *m/z* 184.11 ($M^+$).

**3. Synthesis of Hydroxy Derivatives of $MPP^+$.** All hydroxyl derivatives of $MPP^+$ were obtained by O-demethylation of the corresponding -OMe derivatives of 4-phenylpyridine according to the procedure of Das et al.[11] followed by N-methylation of pyridine nitrogen with $CH_3I$ (Scheme 2). Briefly, a mixture of 10 mL of pyridine and excess concentrated HCl in a three necked flask fitted with a thermometer was heated up to 180 °C until complete removal of water. Then the salt solution was cooled to 140 °C, and 1.0 g of the corresponding methoxy−MPP derivative was added, and the mixture was heated to 200 °C under $N_2$ while stirring for 3 h. The resulting brown solution was cooled to room temperature, and 1 M NaOH was added dropwise until the formation of an orange yellow precipitate was complete. The mixture was stirred for 1 h, and the precipitate was filtered, dissolved in absolute ethanol, and acidified with concentrated HCl. Ethanol was evaporated under vacuum, and the solid was crystallized with ethanol/ether. The resulting solid was filtered, basified with 1% $NaHCO_3$, and extracted into ether. The ether layer was dried over $Na_2SO_4$ and evaporated under vacuum to obtain a white solid. The resulting solid was dissolved in anhydrous THF and cooled to 0 °C, and a 10–20% molar excess of $CH_3I$ was added and stirred for 1 h at 0 °C and for 4 h at room temperature. The resulting light yellow precipitate was filtered and crystallized with ethanol/ether.

**a. 1-Methyl-4-(3′-hydroxyphenyl)pyridinium Iodide (3′-OHM-$PP^+$) (3).** Yield 26%; mp 228–229 °C; $^1$H NMR ($D_2O$) $\delta$ 4.36 (s, 3H), 7.10–7.12 (m, 1H), 7.26 (m, 1H), 7.40–7.49 (m, 2H), 8.16 (d, 2H), 8.71 (d, 2H); $^{13}$C NMR ($D_2O$) $\delta$ 49.7, 117.1, 121.9, 123.1, 127.6, 134.2, 147.5, 158.3, 159.1; MS (ESI) *m/z* 186.6 ($M^+$).

**b. 1-Methyl-4-(4′-hydroxyphenyl)pyridinium Iodide (4′-OHM-$PP^+$) (4).** Yield 23%; mp 222–224 °C; $^1$H NMR ($D_2O$) $\delta$ 4.29 (s, 3H), 7.06 (d, 2H), 7.87 (d, 2H), 8.16 (d, 2H), 8.59 (d, 2H); $^{13}$C NMR ($D_2O$) $\delta$ 49.5, 119.3, 125.8, 127.7, 132.7, 147.08, 157.8, 163.03; MS (ESI) *m/z* 186.6 ($M^+$); Anal. ($C_{12}H_{12}ONI$) C, H, N.

**c. 1,3-Dimethyl-4-(4′-hydroxyphenyl)pyridinium Iodide (6).** Yield 12%; mp 224–226 °C; $^1$H NMR ($D_2O$) $\delta$ 2.48 (s, 3H), 4.31 (s, 3H), 7.03 (d, 2H), 7.46 (d, 2H), 7.83 (d, 1H), 8.25 (d, 1H), 8.61 (s, 1H); $^{13}$C NMR ($D_2O$) $\delta$ 20.3, 49.4, 127.3, 130.3, 132.9, 136.5, 158.2, 162.9; MS (ESI) *m/z* 200.4 ($M^+$); Anal. ($C_{13}H_{14}ONI$) C, H, N.

**4. Synthesis of Hydroxy Derivatives of 1-Methyl-3-phenyl Pyridinium Salts.** A solution of 4-bromoanisole (0.03 mol) in THF was stirred with Mg turnings (0.09 mol) and for 5 h under $N_2$ at

room temperature. The resulting solution was added dropwise to a solution of dichlorobis(triphenylphosphine)nickel(II) and 3-bromopyridine in anhydrous THF and stirred for 12 h under $N_2$. The reaction was quenched by adding diluted HCl, and unreacted starting materials were removed by extracting into $CH_2Cl_2$. The aqueous phase was basified with $NaHCO_3$ and extracted into ether. The ether layer was dried and concentrated under vacuum to obtain a white solid. The solid was dissolved in ethanol, acidified with concentrated HCl, and purified by crystallization with ethanol/ether. The product was O-demethylated and then N-methylated as described for compound **3**, above (Scheme 3).

**a. 1-Methyl-3-(4′-hydroxyphenyl)pyridinium Iodide (13).** Yield 16%; mp 236 °C; $^1$H NMR ($D_2O$) $\delta$ 4.42 (s, 3H), 7.01 (d, 2H), 7.62 (d, 2H), 8.00 (q, 1H), 8.61 (t, 2H), 8.94 (s, 1H); $^{13}$C NMR ($D_2O$) $\delta$ 49.3, 117.1, 121.9, 123.1, 127.6, 134.2, 147.5, 158.3, 162.1; MS (ESI) *m/z* 186.6 ($M^+$); Anal. ($C_{12}H_{12}ONI$) C, H, N.

**b. 1-Methyl-3-(3′-hydroxyphenyl)pyridinium Iodide (14).** Yield 28%; mp 227–229 °C; $^1$H NMR ($D_2O$) $\delta$ 4.26 (s, 3H), 7.10–7.12 (m, 1H), 7.26 (m, 1H), 7.40–7.49 (m, 2H), 8.11 (q, 1H), 8.64 (t, 2H), 8.91 (s, 1H); $^{13}$C NMR ($D_2O$) $\delta$ 49.7, 117.1, 121.9, 122.4, 123.1, 127.6, 129.5, 134.2, 147.5, 158.3, 159.1; MS (ESI) *m/z* 186.6 ($M^+$); Anal. ($C_{12}H_{12}ONI$) C, H, N.

**5. Synthesis of 1-Methyl-4-phenyl-1,2,5,6-tetrahydropyridine (MPTP) Derivatives.** A solution of 1-methyl-4-piperidone (typically 3 mmol scale) in dry THF was mixed with the desired phenyl magnesium bromide and stirred for 12 h at room temperature. The reaction mixture was treated with saturated $NH_4Cl$, and unreacted starting materials were removed by washing with ethyl acetate. The aqueous layer was basified with saturated $NaHCO_3$ and extracted into ether. The ether layer was dried with $Na_2SO_4$ and evaporated to dryness; the residue was dissolved in ethanol, acidified with concentrated HCl, and evaporated to dryness. The product hydrochloride was crystallized with ethanol/ether (Scheme 4).

**a. 1-Methyl-4-(3-hydroxyphenyl)-1,2,3,6-tetrahydropyridine HCl (18).** Yield 23%; $^1$H NMR ($D_2O$) $\delta$ 2.83–3.01 (m, 2H), 3.12 (s, 3H), 3.25–3.32 (m, 1H), 3.66–3.76 (m, 1H), 4.02 (dd, 1H), 4.07 (dd, 1H), 6.13 (dd, 1H), 6.92 (dd, 1H), 6.97 (t, 1H) 7.06–7.08 (m, 1H), 7.35 (t, 1H); $^{13}$C NMR $\delta$ 25.8, 44.3, 50.1, 52.2, 118.7, 125.4, 127.5, 130.3, 132.2, 136.0, 148.7, 159.9; MS (ESI) *m/z* 190.12 ($M^+$).

**b. 1-Methyl-4-(4-hydroxylphenyl)-1,2,3,6-tetrahydropyridine HCl (19).** Yield 32%; $^1$H NMR ($D_2O$) $\delta$ 2.82–2.85 (m, 2H), 3.01 (s, 3H), 3.34 (m, 1H), 3.68–3.74 (m, 1H), 3.78 (dd, 1H), 4.00 (dd, 1H), 6.02 (dd, 1H), 6.91 (d, 2H), 7.41 (d, 2H); $^{13}$C NMR ($D_2O$) $\delta$ 25.5, 44.3, 50.1, 52.5, 117.2, 128.5, 146.3, 148.8, 161.1; MS (ESI) *m/z* 190.12 ($M^+$).

**c. 1-Methyl-4-(3-chlorophenyl)-1,2,3,6-tetrahydropyridine HCl (20).** Yield 41%; $^1$H NMR ($D_2O$) $\delta$ 2.83–3.01 (m, 2H), 3.12 (s, 3H), 3.25–3.32 (m, 1H), 3.66–3.76 (m, 1H), 4.02 (dd, 1H), 4.07 (dd, 1H), 6.13 (dd, 1H), 6.92 (dd, 1H), 6.97 (t, 1H), 7.06–7.08 (m, 1H), 7.35 (t, 1H); $^{13}$C NMR ($D_2O$) $\delta$ 26.4, 44.0, 52.8, 54.2, 118.7, 125.4, 127.5, 130.3, 132.2, 135.6, 136.0, 142.7; MS (ESI) *m/z* 208.19 ($M^+$).

**d. 1-Methyl-4-(4-fluorophenyl)-1,2,3,6-tetrahydropyridine HCl (21).** Yield 36%; $^1$H NMR ($D_2O$) $\delta$ 2.81–2.86 (m, 2H), 3.01 (s, 3H), 3.34 (m, 1H), 3.68–3.74 (m, 1H), 3.78 (dd, 1H), 4.05 (dd, 1H), 6.09 (dd, 1H), 7.18 (t, 2H), 7.51 (q, 2H); $^{13}$C NMR ($D_2O$) $\delta$ 26.4, 44.9, 53.0, 55.2, 117.7, 129.5, 135.3, 136.9, 163.6, 166.1; MS (ESI) *m/z* 192.12 ($M^+$).

**6. Synthesis of $MPP^+$−APP Conjugates.** A mixture of the desired 4-phenylpyridine derivative (6.5 mmol) and excess $NaHCO_3$ in THF was treated with 6.5 mmol of the desired 3-bromo-2-phenylpropene[12] and stirred for 5 h at room temperature (Scheme 5). The solvent was removed under reduced pressure, and the resultant solid was dissolved in absolute ethanol, and insoluble $NaHCO_3$ was removed by filtration. Filtrate was evaporated, and the residue was crystallized with EtOH/ether.

**a. 4-Phenyl-1-(2-phenyl-allyl)pyridinium Bromide (23).** Yield 67%; mp 237–238 °C; $^1$H NMR ($D_2O$) $\delta$ 5.64 (s, 1H), 5.70 (s, 2H), 5.86 (s, 1H), 7.39–7.42 (m, 3H), 7.51–7.55 (m, 4H), 7.80–7.83 (m, 2H), 8.14–8.17 (d, 2H), 8.79–8.82 (d, 2H); $^{13}$C NMR ($D_2O$) $\delta$ 57, 123.8, 127.6, 129.2, 130.6, 131.8, 132.3, 135, 138.8, 143.7, 146.7, 159.6; MS (ESI) *m/z* 272.24 ($M^+$); Anal. ($C_{20}H_{18}BrN$) C, H, N.

**b. 4-Cyclohexyl-1-(2-phenyl-allyl)pyridinium Bromide (24).** Yield 58%; mp 231–232 °C; $^1$H-NMR ($D_2O$) $\delta$ 1.25 (m, 1H), 1.35–1.42 (m, 3H), 1.64–1.83 (m, 4H), 2.80 (t, 1H), 5.56 (s, 1H), 5.63 (s, 2H), 5.81 (s, 1H), 7.35–7.51 (m, 5H), 7.80 (d, 2H), 8.67 (d, 2H); $^{13}$C NMR ($D_2O$) $\delta$ 27.7, 28.3, 34.9, 46.6, 57.0, 66.3, 123.5, 129.1, 129.2, 131.7, 131.8, 138.8, 143.8, 146.1; MS (ESI) *m/z* 348.19 ($M^+$); Anal. ($C_{26}H_{22}BrN$) C, H, N.

**c. 4-(4′-methoxyphenyl)-1-(2-phenyl-allyl)pyridinium Bromide (28).** Yield 74%; mp 241–243 °C; $^1$H NMR ($D_2O$) $\delta$ 3.78 (s, 3H), 5.50 (s, 1H), 5.52 (s, 2H), 5.72 (s, 1H), 6.97 (d, 2H), 7.28 (m, 3H), 7.41 (d, 2H), 7.64 (d, 2H), 7.89 (d, 2H), 8.53 (d, 2H); $^{13}$C NMR ($D_2O$) $\delta$ 38.3, 56.6, 123.9, 128.6, 129.8, 131.6, 132.8, 135.8, 138.8, 143.8, 145.4, 1.58.2, 161.6; MS (ESI) *m/z* 302.15 ($M^+$); Anal. ($C_{21}H_{20}BrNO$) C, H, N.

**d. 4-(3′-hydroxyphenyl)-1-[2-(4-iodophenyl)-allyl]pyridinium Bromide (29).** Yield 46%; mp 245–248 °C; $^1$H NMR ($CD_3OD$) $\delta$ 5.54 (s, 1H), 5.76 (s, 2H), 5.84 (s, 2H), 7.04 (m, 1H), 7.31 (m, 1H), 7.39–7.45 (m, 6H), 8.29 (d, 2H), 8.90 (d, 2H); $^{13}$C NMR ($D_2O$) $\delta$ 64.3, 115.6, 120.2, 120.7, 121.6, 124.2, 126.1, 129.1, 132.1, 133.3, 136.3, 136.8, 142.5, 145.8, 158.8, 160.1; MS (ESI) *m/z* 414.06 ($M^+$); Anal. ($C_{20}H_{17}BrINO$) C, H, N.

**e. 4-(4′-hydroxyphenyl)-1-[2-(4-bromophenyl)-allyl]pyridinium Bromide (30).** Yield 74%; mp 239–240 °C; $^1$H NMR ($D_2O$) $\delta$ 5.48 (s, 1H), 5.72 (s, 2H), 5.74 (s, 1H), 7.24 (d, 2H), 7.26 (d, 2H), 7.44 (d, 2H), 7.87 (d, 2H), 8.21 (d, 2H), 8.76 (d, 2H); $^{13}$C NMR ($D_2O$) $\delta$ 55.7, 63.9, 115.1, 119.3, 122.4, 125.8, 127, 129, 130.7, 134.8, 135.2, 141.3, 144.2, 158.5, 166.4; MS (ESI) *m/z* 366.04 ($M^+$).

**f. 4-Phenyl-1-(2-biphenyl-allyl)pyridinium Bromide (31).** Yield 46%; mp 241–243 °C; $^1$H NMR ($CD_3OD$) $\delta$ 4.95 (s, 1H), 4.98 (s, 2H), 5.15 (s, 1H), 6.64–6.71 (m, 4H), 6.78–6.81 (m, 6H), 6.83–6.85 (m, 4H), 7.68 (d, 2H), 8.32 (d, 2H); $^{13}$C NMR ($CD_3OD$) $\delta$ 57.0, 123.5, 129.1, 129.2, 131.7, 131.8, 132.4, 133.5, 133.8, 138.8, 143.8, 156.1; MS (ESI) *m/z* 348.19 ($M^+$); Anal. ($C_{26}H_{22}BrN$) C, H, N.

**g. 4-Phenyl-1-(2-phenyl-allyl)piperidine Chloride (25).** Yield 31%; mp 224–226 °C; $^1$H NMR ($D_2O$) $\delta$ 3.53 (br s, 9H), 4.41 (s, 2H), 5.72 (s, 1H), 5.87 (s, 1H), 7.17–7.20 (m, 3H), 7.41–7.59 (m, 7H); $^{13}$C NMR ($D_2O$) $\delta$ 47.7, 50.9, 60.2, 118.3, 124.3, 125.2, 126.7, 129.3, 130, 137.3, 137.4, 146.9; MS (ESI) *m/z* 278.19 ($M^+$).

**h. 4-Phenyl-1-(2-phenyl-allyl)pyrimidine Hydrochloride (26).** Yield 34%; $^1$H NMR ($D_2O$) $\delta$ 5.71 (s, 1H), 5.72 (s, 2H), 5.91 (s, 1H), 7.39–7.54 (m, 4H), 7.54–7.61 (m, 5H), 7.64–7.73 (m, 1H), 8.21 (d, 2H), 8.41 (d, 1H), 9.07 (dd, 1H), 9.56 (s, 1H); $^{13}$C NMR ($D_2O$) $\delta$ 56.8, 57.9, 119.3, 124.3, 125.2, 126.7, 129.3, 130, 137.3, 137.4, 156.9; MS (ESI) *m/z* 273.19 ($M^+$).

**i. 4-Phenyl-1-(2-phenyl-allyl)piperazine Hydrochloride (27).** Yields 34%; mp 212–214 °C; $^1$H NMR ($D_2O$) $\delta$ 4.24 (br s, 8H), 5.12 (s, 2H), 5.62 (s, 1H), 5.89 (s, 1H), 7.17–7.20 (m, 3H), 7.41–7.59 (m, 7H); $^{13}$C NMR ($D_2O$) $\delta$ 49.7, 52.7, 60.8, 119.6, 125.8, 126.4, 126.7, 129.8, 133.5, 137.8, 137.2, 146.9; MS (ESI) *m/z* 279.19 ($M^+$); Anal. ($C_{19}H_{23}ClN_2$) C, H, N.

**Acknowledgment.** This work was supported by the National Institutes of Health (NS 39423).

**Supporting Information Available:** Elemental analysis data of compounds **4**, **6**, **13**, **14**, **23**–**24**, **27**–**29**, and **31**. This material is available free of charge via the Internet at http://pubs.acs.org.

## References

(1) Gerlach, M.; Riederer, P.; Przuntek, H.; Youdim, M. B. MPTP mechanisms of neurotoxicity and their implications for Parkinson's disease. *Eur. J. Pharmacol.* **1991**, *208*, 273–286.

(2) Tipton, K. F.; Singer, T. P. Advances in our understanding of the mechanisms of the neurotoxicity of MPTP and related compounds. *J. Neurochem.* **1993**, *61*, 1191–1206.

(3) Fiskum, G.; Starkov, A.; Polster, B. M.; Chinopoulos, C. Mitochondrial mechanisms of neural cell death and neuroprotective interventions in Parkinson's disease. *Ann. N.Y. Acad. Sci.* **2003**, *991*, 111–119.

(4) Obata, T. Dopamine efflux by MPTP and hydroxyl radical generation. *J. Neural Transm.* **2002**, *109* (9), 1159–1180.
(5) Kahlig, K. M.′; Galli, A. Regulation of dopamine transporter function and plasma membrane expression by dopamine, amphetamine, and cocaine. *Eur. J. Pharmacol.* **2003**, *479*, 153–8.
(6) Torres, G. E. The dopamine transporter proteome. *J. Neurochem.* **2006**, *97*, 3–10.
(7) Daniels, A. J.; Reinhard, J. F., Jr. Energy-driven uptake of the neurotoxin 1-methyl-4-phenylpyridinium into chromaffin granules. *J. Biol. Chem.* **1988**, *263*, 5034–5036.
(8) Darchen, F.; Scherman, D.; Henry, J.-P. Characteristics of the transport of quaternary ammonium 1-methyl-4-phenylpyridinium by chromaffin granules. *Biochem. Pharmacol.* **1988**, *37*, 4381–4387.
(9) Das, A.; Jeffery, J. C.; Maher, J. P.; McCleverty, J. A.; Schatz, E.; Ward, M. D.; Wollermann, G. Mono- and binuclear molybdenum and tungsten complexes containing asymmetric bridging ligands: effects of ligand conjugation and conformation on metal−metal interactions. *Inorg. Chem.* **1993**, *32*, 2145–2155.
(10) Arora, P. K.; Riachi, N. J.; Fiedler, G. C.; Singh, M. P.; Abdallah, F.; Harik, S. I.; Sayre, L. M. Structure−neurotoxicity trends of analogues of 1-methyl-4-phenylpyridinium ($MPP^+$), the cytotoxic metabolite of the dopaminergic neurotoxin MPTP. *Life Sci.* **1990**, *46*, 379–390.
(11) Das, A.; Jeffery, J. C.; Maher, J. P.; McCleverty, J. A.; Schatz, E.; Ward, M. D.; Wollermann, G. *Angew. Chem., Int. Ed. Engl.* **1992**, *31*, 1515–1518.
(12) Perera, R. P.; Wimalasena, D. S.; Wimalasena, K. Characterization of a series of 3-amino-2-phenylpropene derivatives as novel bovine chromaffin vesicular monoamine transporter inhibitors. *J. Med. Chem.* **2003**, *46*, 2599–2605.
(13) Wimalasena, D. S.; Wimalasena, K. Kinetic evidence for the channeling of dopamine between monoamine transporter and membranous dopamine $\beta$-monooxygenase in chromaffin granule ghosts. *J. Biol. Chem.* **2004**, *279*, 15298–15304.
(14) Wimalasena, K.; Wimalasena, D. S. The reduction of membrane-bound dopamine $\beta$-monooxygenase in resealed chromaffin granule ghosts: is intra-granular ascorbic acid a mediator for the extra-granular reducing equivalents. *J. Biol. Chem.* **1995**, *270*, 27516–27524.
(15) Henry, J. P.; Botton, D.; Sagne, C.; Isambert, M. F.; Desnos, C.; Blanchard, V.; Raisman Vozari, R.; Krejci, E.; Massoulie, J.; Gasnier, B. Biochemistry and molecular biology of the vesicular monoamine transporter from chromaffin granules. *J. Exp. Biol.* **1994**, *196*, 251–262.
(16) Darchen, F.; Scherman, D.; Henry, J.-P. Reserpine binding the chromaffin granules suggests the existence of two conformations of the monoamine transporter. *Biochemistry* **1989**, *28*, 1692–1697.
(17) Scherman, D.; Henry, J.-P. Effect of drugs on the ATP-induced and pH-gradient-driven monoamine transport by bovine chromaffin granules. *Biochim. Biophys. Acta* **1980**, *601*, 664–677.
(18) Darchen, F.; Scherman, D.; Laduron, P. M.; Henry, J.-P. Ketanserin binds to the monoamine transporter of chromaffin granules and of synaptic vesicles. *Mol. Pharmacol.* **1988**, *33*, 672–677.
(19) Parti, R.; Ozkan, E. D.; Harnadek, G. J.; Njus, D. Inhibition of norepinephrine transport and reserpine binding by reserpine derivatives. *J. Neurochem.* **1987**, *48*, 949–953.
(20) Chaplin, L.; Cohen, A. H.; Huettl, P.; Kennedy, M.; Njus, D.; Temperley, S. J. Reserpic acid as an inhibitor of norepinephrine transport into chromaffin vesicle ghosts. *J. Biol. Chem.* **1985**, *260*, 10981–10985.
(21) Frisch, M. J.; Trucks, G. W.; Schlegel, H. B.; Scuseria, G. E.; Robb, M. A.; Cheeseman, J. R.; Zakrzewski, V. G.; Montgomery, J. A., Jr.; Stratmann, R. E.; Burant, J. C.; Dapprich, S.; Millam, J. M.; Daniels, A. D.; Kudin, K. N.; Strain, M. C.; Farkas, O.; Tomasi, J.; Barone, V.; Cossi, M.; Cammi, R.; Mennucci, B.; Pomelli, C.; Adamo, C.; Clifford, S.; Ochterski, J.; Petersson, G. A.; Ayala, P. Y.; Cui, Q.; Morokuma, K.; Malick, D. K.; Rabuck, A. D.; Raghavachari, K.; Foresman, J. B.; Cioslowski, J.; Ortiz, J. V.; Baboul, A. G.; Stefanov, B. B.; Liu, G.; Liashenko, A.; Piskorz, P.; Komaromi, I.; Gomperts, R.; Martin, R. L.; Fox, D. J.; Keith, T.; Al-Laham, M. A.; Peng, C. Y.; Nanayakkara, A.; Challacombe, M.; Gill, P. M. W.; Johnson, B.; Chen, W.; Wong, M. W.; Andres, J. L.; Gonzalez, C.; Head-Gordon, M.; Replogle, E. S.; Pople, J. A. *Gaussian 98,* Revision-A.9; Gaussian, Inc.: Pittsburgh, PA, 1998.
(22) Przedborski, S.; Jackson-Lewis, V.; Naini, A. B.; Jakowec, M.; Petzinger, G.; Miller, R.; Akram, M. The parkinsonian toxin 1-methyl-4-phenyl-1,2,3,6-tetrahydropyridine (MPTP): A technical review of its utility and safety. *J. Neurochem.* **2001**, *76*, 1265–1274.
(23) Cleland, W. W. Statistical analysis of enzyme kinetic data. *Methods Enzymol.* **1979**, *63*, 103–138.

JM070875P